Liquid Mixing in a Tapered Fluidized Bed

George H. Webster,
Joseph J. Perona
Department of Chemical Engineering
University of Tennessee
Knoxville, TN 37996-2200

Some aspects of the hydrodynamics of a two-phase (liquid-solid) tapered fluidized bed were explored for applications in the modeling and development of bioreactors in which microorganisms are immobilized on solids and contacted by liquid nutrient streams. Both tapered and cylindrical fluidized beds have been used in this capacity (Lee et al., 1979; Jeris et al., 1977). Two-phase tapered fluidized beds also have both laboratory and industrial applications as crystallizers (Ishii, 1973; Permutit Co., Inc., 1975). One advantage of the tapered bed over the cylindrical bed in these applications is its ability to fluidize a wider range of particle sizes.

In order to evaluate tapered fluidized beds for such applications, necessary modeling information such as liquid dispersion (fluid mixing), bed expansion, and particle segregation were determined and compared with similar measurements in a cylindrical fluidized bed. Axial dispersion coefficients were measured in both fluidized beds using an imperfect pulse salt tracer technique. Void fractions were also measured at many axial positions in the tapered fluidized bed using an electrical resistance technique and were compared to the Wen and Yu (1966) void fraction correlation for cylindrical fluidized beds. Experiments with a size distribution of coal particles indicated that particle segregation was greater in a cylindrical bed than in a tapered bed. More detail is given by Webster and Perona (1987).

A general correlation for axial dispersion coefficients in cylindrical two-phase (liquid-solid) fluidized beds, which includes the effects of velocity, particle size, and column diameter, does not exist. The literature indicates that axial dispersion coefficients for cylindrical fluidized beds generally increase as velocity or void fraction increases and increase as particle size increases at similar void fractions.

Experiments were done with a tapered column 106.7 cm in length, with an overall taper angle of 1.47°. The column size increased from 2.54 cm ID at the bottom to 7.62 cm at the top. Seven glass ports, 0.5 cm in diameter and sealed with rubber septums, were evenly spaced along the column. A port 18.5 cm above the column base was used for the tracer injection. The flow entrance region of the tapered column consisted of a 1 cm ID pipe connected to a stainless steel plate with a 1.2 cm hole in the center. A wire mesh screen covered the plate and both were fastened to the bottom of the column. The screen supported the particles and prevented spouting of fluid in the center of the column.

The cylindrical column was 5.08 cm in diameter and 110 cm in height. Four glass ports, 0.5 cm in diameter and sealed with rubber septums, were spaced along the column. The flow entrance region was similar to that for the tapered column with a screen to suppress spouting.

Usually 630 cm^3 of coal or 430 cm^3 of glass particles were fluidized in the columns. The anthracite coal particles were a mixture between 30 mesh (0.025 cm) and 60 mesh (0.059 cm) with a density of 1.53 g/cm^3. The glass beads, purchased from Thomas Scientific, ranged from 0.01 to 0.012 cm in diameter with a density of 2.76 g/cm^3. The average particle diameters were determined to be 0.032 cm for coal and 0.010 cm for glass by a best fit of the cylindrical column void fraction data using the correlation of Wen and Yu (1966).

Tracer concentration measurements were made by injecting sodium nitrate solution with a syringe through the rubber septums. Concentration measurements were made with a probe connected to an impedance bridge especially designed to provide a fast response time. Details of the apparatus and procedure are given by Webster (1986).

Dispersion Results

Particle motions were observed at the walls of both the tapered and cylindrical columns by fluidizing glass particles with a trace of coal particles present. Since the glass appeared white, the particle motions at the walls could be observed by following the motions of the black coal particles. A downward flow of particles was observed at the walls of the tapered column, while random particle motion was observed at the walls of the cylindrical column. Dye was injected into the tapered column

Correspondence concerning this paper should be addressed to J. J. Perona.

during glass particle fluidization, at points near the wall where the particles flowed downward. The dye also flowed downward and then mixed radially. The downward flow was also observed in coal fluidization but to a lesser extent than in glass fluidization. The downward flow velocity was approximately 2 cm/s for coal fluidization and 5 cm/s for glass fluidization; these compare to Stokes law settling velocities of 3 and 1 cm/s, respectively. This downward flow decreases the cross-sectional area available for upward flow and increases the upward flow rate of fluid (the upward flow rate being larger than the flow rate entering the column). Furthermore, this downward flow is a characteristic of the conical shape and not of the distributor, as was proven by attaching a pipe (60 cm length, 2.54 cm dia.) to the entrance of the tapered column. The pipe was packed with 0.3 cm glass beads, and according to Cairns and Prausnitz (1959) this entrance region should provide a flat velocity profile. The flow patterns were unchanged using this entrance region.

Experimental data for all runs are presented in Table 1. The mean residence time was calculated as the difference between the mean times, μ, of the upstream and downstream concentration vs. time response curves:

$$\mu = \frac{\int_0^\infty tC\,dt}{\int_0^\infty C\,dt} \tag{1}$$

The mean residence time was essentially the same (within approximately 6%) as the difference between the median times of the response curves, where the median time is the time at which 50% of the tracer mass has passed the measuring probe. Mass balances were performed for all response curves and there was good agreement (within 10%) between upstream and downstream measuring points. Variances were calculated for each

Table 1. Experimental Conditions, Residence Times, and Dispersion Coefficients

Run No.	Flow Rate mL/s	Quantities Evaluated Between Measurement Points: Vol.-Weighted Superfic. Veloc. cm/s	Vol.-Weighted Void Frac.	Length cm	Residence Times: Plug-flow s	Residence Times: Mean s	Dispersion** Coeff. cm^2/s
			Tapered Column Coal Runs				
1	8.3	0.33	0.666	28.5	48.0	14.5	53.6†
2	8.3	0.33	0.657	24.7	42.6	6.7	232.5†
3	11.5	0.43	0.708	31.5	45.5	18.6	30.7†
4	13.4	0.50	0.721	33.5	42.9	20.1	12.3
5	18.6	0.66	0.768	40.0	41.3	26.4	8.7
6	21.2	0.72	0.762	45.6	43.9	26.8	13.1
7	25.0	0.85	0.794	45.5	37.4	27.9	12.6
8	30.9	1.00	0.818	54.5	40.0	28.9	7.7
9	32.2	1.03	0.803	55.9	38.5	31.3	12.1
10a*	35.3	1.39	0.856	27.0	14.8	16.2	13.1
10b	35.3	1.15	0.828	53.4	34.2	28.8	12.6
10c	35.3	0.98	0.808	26.4	19.4	13.1	12.3
11	39.3	1.22	0.840	59.8	36.8	29.0	12.3
			Cylindrical Column Coal Runs				
12	8.3	0.41	0.678	20.0	30.9	40.6	5.4
13	9.6	0.48	0.702	26.1	36.4	35.3	6.3
14	13.4	0.66	0.765	39.0	42.4	35.7	3.4
15	16.0	0.79	0.789	45.6	44.1	41.4	5.3
16	18.6	0.92	0.818	59.5	50.2	43.8	1.5
17a*	21.2	1.04	0.848	36.0	27.6	24.0	4.3
17b	21.2	1.04	0.848	71.6	54.8	51.9	3.8
17c	21.2	1.04	0.848	35.6	27.2	28.0	3.4
18	31.5	1.55	0.912	56.8	32.0	32.0	3.1
			Tapered Column Glass Runs				
19	8.3	0.31	0.748	33.6	71.8	34.3	7.7
20	11.5	0.41	0.799	41.3	70.2	36.8	8.8
21	13.4	0.46	0.817	46.3	72.9	42.9	9.6
22	14.7	0.49	0.831	48.7	72.3	44.3	7.2
23	18.6	0.60	0.861	56.0	71.8	47.1	8.7
			Cylindrical Column Glass Runs				
24	6.7	0.33	0.790	41.7	94.9	78.2	1.2
25	8.3	0.41	0.854	70.0	138.5	122.2	1.0
26	10.3	0.51	0.875	30.0	49.5	36.7	1.5
27	11.5	0.57	0.910	48.5	74.0	62.9	0.9

*a, b, c: upstream-midstream, upstream-downstream, midstream-downstream measuring points, respectively.
**Tapered column dispersion coefficients calculated using mean residence time
†These large dispersion coefficients are not included in Figure 2 because, at these low flow rates, complete fluidization was not achieved

upstream and downstream curve:

$$\sigma^2 = \frac{\int_0^\infty t^2 C\, dt}{\int_0^\infty C\, dt} - \mu^2 \tag{2}$$

and the dimensionless variance differences were obtained:

$$\sigma_\infty^2 = \frac{\sigma_2^2 - \sigma_1^2}{\bar{t}^2} \tag{3}$$

Plug-flow residence times (calculated as the volume divided by the flow rate) were found to be consistently larger than mean residence times in the tapered fluidized bed and approximately the same as mean residence times in the cylindrical fluidized bed, Table 1. This shows that the tapered fluidized bed is characterized by fluid channelling in the center with downward flow or stagnant regions at the walls; this flow pattern is markedly different than the flow pattern in the cylindrical fluidized bed.

Dispersion coefficients were calculated from the dimensionless variance difference as presented by Bischoff and Levenspiel (1962):

$$D = \bar{v} L\, \sigma_\infty^2 / 2 \tag{4}$$

For the tapered column the volume-weighted superficial velocity (Eq. 5, below) was used as the velocity between the two measurement points and the volume-weighted void fraction (calculated using Eq. 5, substituting void fraction for velocity) was used as the average void fraction between the two measurement points.

The dispersion coefficients measured in the cylindrical fluidized bed were of the same magnitude as literature dispersion coefficients and decreased as particle size decreased, as do literature dispersion coefficients, but did not increase with velocity as do most literature studies. We note that most of the literature data are for larger particles, which may not fluidize homogeneously. Data on small particles were presented by Bruinzeel et al. (1962) and Muchi et al. (1961). Bruinzeel et al. fluidized sand mixtures with average diameters between 0.02 and 0.03 cm in a 100 cm column in which the fluidization was observed to be smooth. The dispersion coefficients increased from 2.1 to 6.3 cm^2/s as void fraction increased from 0.58 to 0.87. Muchi et al. fluidized sand mixtures with average diameters between 0.031 and 0.084 cm and found almost no increase in dispersion coefficients as void fraction increased within the experimental scatter.

Experimental dispersion coefficients in the cylindrical fluidized bed are compared with the correlation of Bruinzeel et al. in Figure 1 as the Peclet number, N_{Pe}, vs. the particle Reynolds number, N_{Re}, where both dimensionless numbers are based on the interstitial velocity.

Dispersion coefficients for the tapered column were calculated using mean residence times. These tapered fluidized bed dispersion coefficients do not appear to depend on void fraction, Figure 2. The average values for the tapered fluidized bed dispersion coefficients are 12.5 cm^2/s for the coal and 8.4 cm^2/s for the glass. Although the dispersion coefficients for the coal are larger than for glass, the dependence is not to the inverse of the particle diameter, as was found for the cylindrical fluidized bed dispersion coefficients. We must note that the one-parameter axial dispersion model is probably not applicable to the tapered fluidized bed because of the stagnant and downward flow regions at the wall. We use the axial dispersion model as a basis

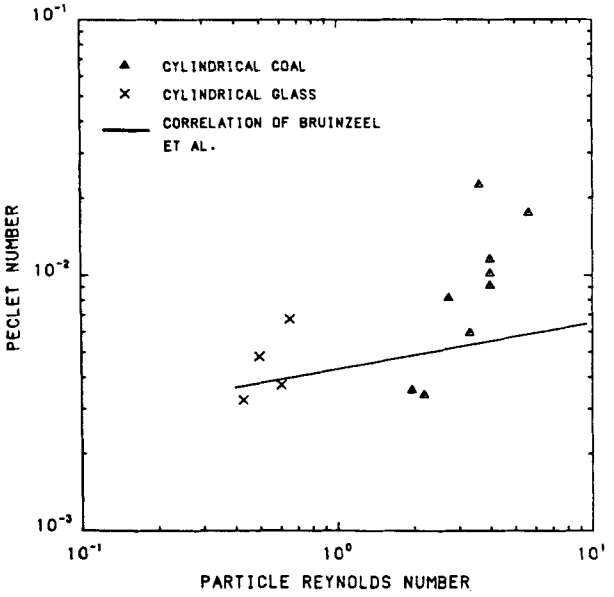

Figure 1. Experimental axial dispersion coefficients for cylindrical fluidized bed compared with correlation of Bruinzeel et al. (1962).

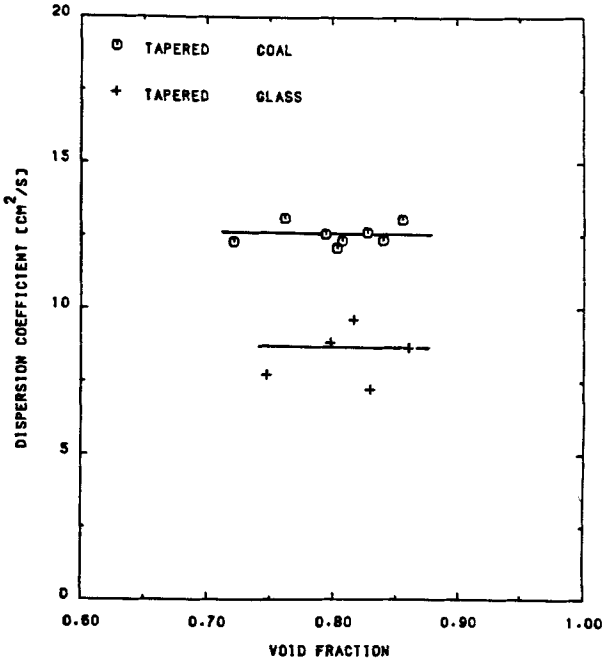

Figure 2. Axial dispersion coefficients vs. void fraction for tapered column fluidizing both coal and glass.

Coefficients calculated using mean residence time

Table 2. Downward Flow Estimations in the Tapered Fluidized Bed

Category	% of Total Vol. Occupied by Downward Flow Regions	Downward Flow Rate as % of Entering Flow Rate
Coal fluidization at small void fractions (Runs 1–4)	40	0 (stagnant)
Coal fluidization at large void fractions (Runs 5–11)	15	15
Glass fluidization (Runs 19–24)	10	60

of comparison of the fluid mixing between the tapered and cylindrical fluidized beds. The axial dispersion model appears to be applicable to the cylindrical fluidized bed since the plug-flow and mean residence times are equal.

A recycle reactor type flow model, which consisted of an upward and downward flow vessel, was used in order to estimate the magnitude of the downward flow in the tapered fluidized bed. The length between the measuring probes divided by the mean residence time was used as the velocity in the upward flow vessel and the downward velocity measured at the walls of the tapered column was used as the velocity in the downward flow vessel. The portion of the vessel occupied by each flow region was calculated by mass balance using the estimated velocities. The model results were divided into three categories and are presented in Table 2. Downward flow did not occur for coal particle fluidization at small void fractions. Instead, stagnant liquid regions of particles slowly moving downward were observed at the walls of the tapered column, while fast-moving fluid in the center of the column provided most of the upward flow. The downward flow region at the walls and the channelling region in the center of the column were small for coal particle fluidization at large void fractions. Only 15% of the cross-sectional area was occupied by the downward flow region. For glass particle fluidization the volume occupied by the downward flow was small, but the amount of downward flow was large. Glass particle fluidization is therefore characterized by a thin layer of fast-moving downward flow at the column walls.

Void Fraction Results

The overall bed expansion data for the tapered and cylindrical columns, fluidizing both coal and glass, are presented in a plot of superficial velocity vs. void fraction in Figure 3. The volume-weighted superficial velocity, $\bar{v}_{ow}$, was used as the superficial velocity in the tapered column and is defined by

$$\bar{v}_{ow} = \int_0^{V_T} \frac{v_o(V)\,dV}{V_T} = \sum_{i=1}^{n} \frac{v_{oi}\Delta V}{V_T} \tag{5}$$

where V is the volume and V_T is the total fluidized volume. In Eq. 5 the integral was approximated by a summation over the total fluidized volume, where n is the number of volume intervals, and the superficial velocity at each axial position, v_{oi}, was found by dividing the volumetric flow rate by the column cross-sectional area at that position. The volume-weighted superficial

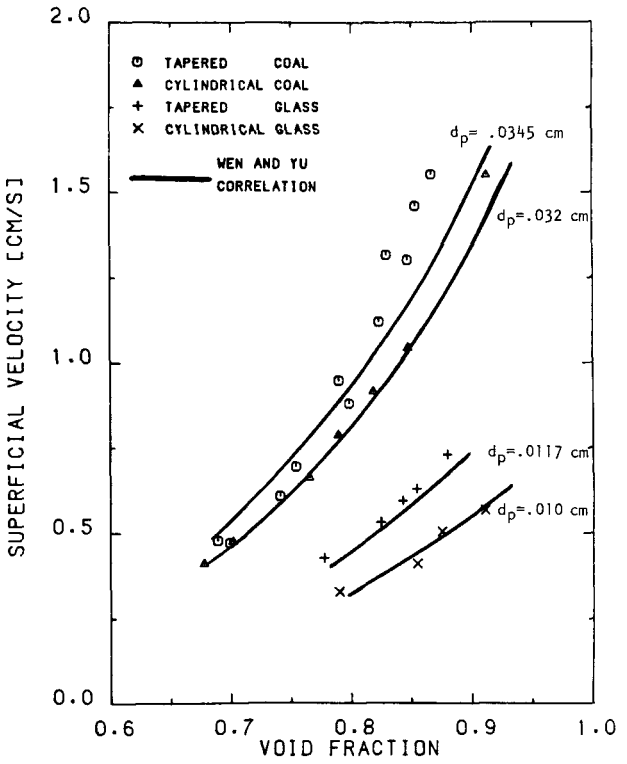

Figure 3. Superficial velocity vs. overall void fraction for both tapered and cylindrical columns fluidizing coal and glass.

Tapered superficial velocities calculated using volume-weighted superficial velocity

velocity is a suitable average velocity to use for the tapered bed because it yields the same overall void fraction in the Wen and Yu correlation as the summed local void fractions calculated with local velocities. The void fractions in Figure 3 were calculated as the total void volume divided by the total fluidized volume and are termed overall void fractions in order to distinguish them from the local void fractions at each axial position in the tapered column.

Local void fractions were found at many axial positions in the tapered column, Figure 4, by measuring the combined resistance of both coal particles and water between the probe wires, using the resistance balance on the impedance bridge. Resistance measurements were converted to void fractions using an empirical correlation obtained with known void fractions in the cylindrical fluidized bed. This method was similar to that used by Maruyama et al. (1984).

The data in Figures 3 and 4 show that the tapered bed fluidizes more densely than the cylindrical fluidized bed. In some cases the difference is as much as 7%. Maruyama et al. also found this trend in tapered channels of 1.9° and larger fluidizing 0.05 cm to 0.35 cm glass beads. We correlate the local void fraction data in Figure 4 by a modified form of the Wen and Yu correlation (1966),

$$\epsilon = \left(\frac{10.6N_{Re} + 1.59N_{Re}^{1.687}}{N_{Ga}}\right)^{0.145} \tag{6}$$

Volume-weighted void fractions calculated using Eq. 6 are closer to the experimental overall void fractions, Figure 3, than

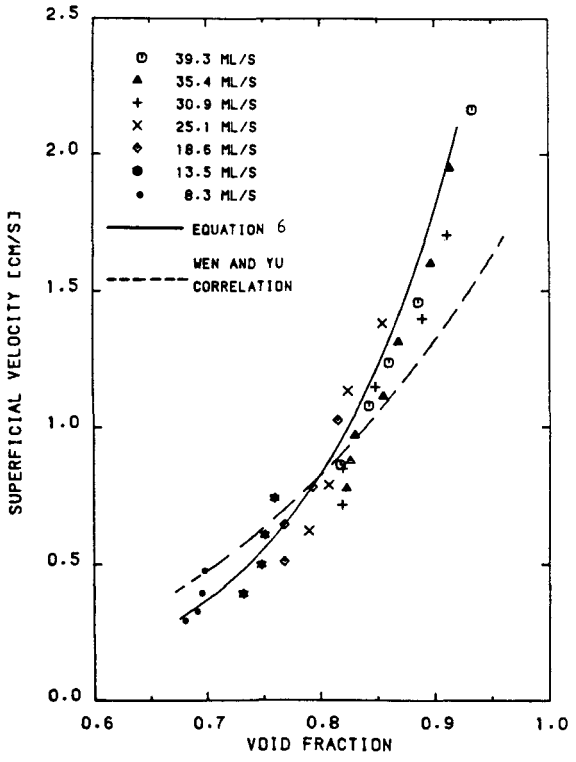

Figure 4. Local void fraction data in tapered column fluidizing coal particles presented as superficial velocity vs. void fraction.

those calculated using the Wen and Yu correlation for both coal and glass fluidization.

Acknowledgment

The authors are grateful to Texaco USA for support of this research through the Texaco Fellowship in Chemical Engineering.

Notation

C = concentration, mol/cm^3
d_p = particle diameter, cm
D = axial dispersion coefficient, cm^2/s
L = axial distance between measuring points, cm
n = number of axial positions
N_{Ga} = Galileo number, $d_p^3\rho(\rho_p - \rho)g/\eta^2$
N_{Pe} = Peclet number, $d_p\bar{v}/D$
N_{Re} = particle Reynolds number, $d_p\bar{v}/\nu$ or $d_p\bar{v}_o/\nu$
t = time, s
$\bar{t}$ = average residence time of fluid between upstream and downstream measurement points, s
$\bar{v}$ = average interstitial velocity, $\bar{v}_o/\epsilon$, cm/s
$\bar{v}_o$ = average superficial velocity, cm/s
v_{oi} = superficial velocity at each axial position in tapered column, cm/s
$\bar{v}_{ow}$ = volume-weighted superficial velocity, characteristic superficial velocity in tapered fluidized bed, cm/s
V_T = total fluidized volume, cm^3

Greek letters

μ = mean or first moment of concentration vs. time response curves, s
ν = kinematic viscosity, cm^2/s
σ^2 = variance or second moment of concentration vs. time response curves, s^2

Subscripts

1 = upstream measuring point
2 = downstream measuring point
∞ = dimensionless quantity

Literature Cited

Bischoff, K. B., and O. Levenspiel, "Fluid Dispersion—Generalizations and Comparison of Mathematical Models. I: Generalized Models," *Chem. Eng. Sci.*, **17,** 245 (1962).

Bruinzeel, C., G. H. Reman, and E. Th. Van der Laan, "Eddy Diffusion in Particulate Fluidized Beds: Model Experiments for the Design of a Large-Scale Unit," *3rd Cong. Eur. Fed. Chem. Eng.*, Olympia, London (June, 1962).

Cairns, E. J., and J. M. Prausnitz, "Velocity Profiles in Packed and Fluidized Beds," *Ind. Eng. Chem.*, **51,** 1441 (1959).

Ishii, T., "Multi-Particle Crystal Growth Rates in Vertical Cones," *Chem. Eng. Sci.*, **28,** 1121 (1973).

Jeris, J. S., R. W. Owens, R. Hickey, and F. Flood, "Biological Fluidized-Bed Treatment for BOD and Nitrogen Removal," *J. Water Pollut. Control Fed.*, **49,** 816 (1977).

Lee, D. D., C. D. Scott, and C. W. Hancher, "Fluidized-Bed Bioreactor for Coal Conversion Effluents," *J. Water Pollut. Control Fed.*, **51,** 974 (1979).

Maruyama T., H. Maeda, and T. Mizushina, "Liquid Fluidization in Tapered Vessels," *J. Chem. Eng. (Japan)*, **17,** 132 (1984).

Muchi, I., T. Mamuro, and K. Saski, "Studies on the Mixing of Fluid in Fluidized Beds," *Chem. Eng. (Japan)*, **25,** 747 (1961).

Permutit Company, Inc., "The Permutit Spiractor," Bull. 5852, Paramus, NJ (1975).

Webster, G. H., "Hydrodynamic Comparison Between a Tapered and a Cylindrical Fluidized Bed by Measurement of Liquid Dispersion, Bed Expansion, and Particle Segregation," Master's Thesis, Univ. Tennessee, Knoxville (1986).

Webster, G. H., and J. J. Perona, "Liquid Mixing in a Tapered Fluidized Bed," AIChE Meet., New York (Nov., 1987).

Wen, C. Y., and Y. H. Yu, "Mechanics of Fluidization," *Chem. Eng. Prog. Symp. Ser.*, **62,** 100 (1966).

Manuscript received July 15, 1987, and revision received Feb. 18, 1988.